Multi – vs. Single – Perceptron Approach for Modelling the Pattern Recognition and Classification in a Multi-Compartment Adaptive Immune System Model

Stephan Scheidegger[1], Rudolf M. Füchslin[1] and Udo S. Gaipl[2]

[1] ZHAW School of Engineering, Zurich University of Applied Sciences, Winterthur, Switzerland
[2] Translational Radiobiology, Department of Radiation Oncology, Universitätsklinikum Erlangen, Germany

scst@zhaw.ch

Abstract

The computer simulation of tumor – host ecosystems interacting with an adaptive immune system may serve as a tool for anti-cancer treatment optimization, but requires appropriate mathematical models. Regarding the tasks of the adaptive immune system (antigen pattern recognition and classification), a perceptron can be used as a conceptual structure representing corresponding biological structures for antigen pattern recognition and classification such as Antigen Presenting Cells (APC's) and their interaction with effector cells in lymph nodes. Regarding the topology of the lymph vessel network, the adaptive immune system may be represented by several perceptrons receiving information about antigen patterns from different tissue compartments. In this study, two scenarios of lymph node arrangement have been investigated. In both scenarios, a tumor-host tissue compartment is treated with ionizing radiation and a second compartment with host tissue and a tumor metastasis is not irradiated. The results exhibit a dependence of the immune response onto the lymph node arrangement, indicating that the topology of the lymph node network is important for an optimal adaptive immune response. The presented simplistic model structure does not allow for a perfect classification between tumor and host tissue. Instead of a single perceptron which is related to the interaction of immune cells in a corresponding lymph node as suggested in this study, networks of locally interacting units may be considered as layers building a deep (convolutional) neural network - like structure.

Introduction

In analogy to the neuronal system, the (adaptive) immune system can be considered as an information-processing system (Fig.1). Assuming a coupling between different information processing systems seems plausible: The immune system acquires detailed information about the chemical structure of an entity regarded as the goal of attacks. The neuronal system often gathers precise information about the location of the problem (e.g. a wound). The mental level could provide further, potentially helpful information, such as the cause of the problem (contact with a specific animal species, insect bite etc.). The information processing in the immune system occurs on the basis of cells that can move and migrate to fulfil their functions in the appropriate micro-environment. In contrast to the central nervous system, pattern recognition and classification are not carried out by neurons in a more or less fixed network structure but in a sort of fluid network. Thereby, the term "fluid" has various meanings. First, the immune system is not bound to a matrix or form some sort of (solid) tissue (except lymphoid organs). The relative position of interacting components (e.g. dendritic cells or effector cells) can change, like that of the particles in a fluid. A second interpretation refers to the interaction between these components: the couplings are specific, but develop on various time scales (cells only interact, if they are in proximity and on a longer time scale, their interaction reflects the adaptivity of the system).

Regarding anti-cancer treatments, the perspective of an information processing element in a tumor-host ecosystem may support novel approaches for therapy optimizations or the design of improved therapies (Scheidegger et al., 2021). In this context, Scheidegger et al., 2020, already proposed a model for a coupled immune – tumor – host ecosystem and demonstrated the feasibility of coupling an ecosystem model with an information processing unit with the structure and function of a perceptron for antigen pattern recognition and classification. In contrast to other models for adaptive immune systems using ordinary differential equation (ODE) systems in the context or viral infections (Du & Yuan, 2020; Leon et al., 2023), the effect of immunogenic memory (Wyatt & Levy, 2020) or tumor-immune system interactions (Chrobak, & Herrero, 2011), such a model can be used as an artificial system to explore the fundamental dynamics when pattern-detecting / classifying and learning components interact with complex ecosystems. However, the systems investigated so far by Scheidegger et al. (2020, 2021) consist of a tumor-host ecosystem which is coupled to only one perceptron. The mapping of this structure onto a real biological system (patient) remains unclear. It can be assumed that the proposed system describes more a local than a systemic adaptive immune response. A further shortcoming of the model is the use of a single tumor – host compartment. In a real patient, many different compartments with (different) host tissues and - in case of tumor metastasis - with smaller populations of tumor sub-clones contribute to the antigen signatures seen by the adaptive immune system. A model including different compartments would allow the investigation of the so-called

abscopal effect (tumor cell elimination in distant, not-treated - respectively not irradiated - organs by the immune system based on a local immune response in the treated (irradiated) organ / compartment, summarized in Frey et al., 2012).

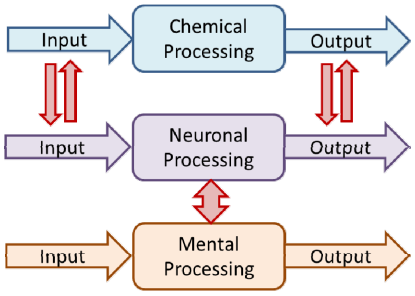

Figure 1. Information processing on different levels: On the level of the (adaptive) immune system, information is encoded chemically (by molecules such as antigen pattern, danger signals, cytokines). In analogy to the neuronal level, this chemically encoded information has to be processed by the immune system. The task of pattern recognition and classification can be modelled by a perceptron, which is then considered as a fundamental unit of information processing similar to the neuronal system. The function of an immunological perceptron may be implemented by specific cells (starting with Antigen Presenting Cells, in combination with other immune cells interacting in the lymph nodes or tissue compartment); similar to the neuronal system, where neurons are involved. It is assumed that the immune system interacts with the neuronal system by a chemical interaction of the in- and outputs. In contrast to this, the interaction with the mental level occurs by the formation of the dynamic neuronal networks in the brain. In- and output on the mental level are semantic: This semantics has to be encoded first by the neuronal network structures of the brain; therefore, the in- and outputs are assumed to not interact with the neuronal level (but these in- and outputs are encoded by neuronal signals). The authors acknowledge the inspiring discussions with Roland Scholz, ETHZ.

To understand the immune response in general, the spatial aspects of information processing should be included in such models. This raises the question, how the biological system can be mapped to a multi-compartment model using perceptrons as information-processing units. Scheidegger et al., 2022, investigated the influence of the antigen-pattern vector size in a single-compartment model: The results exhibit an anti-host immune response after radiotherapy (RT), which is more pronounced for smaller antigen vector sizes. This result could be interpreted as a local inflammatory reaction after irradiation. However, the anti-host response in the model seems to be based on a lack of information since the danger signal triggering the perceptron response is generated in the same compartment where tumor – and host tissue cell populations with their specific antigen patterns are present. Considering a 2-compartment model (one irradiated tumor-host compartment and a second, non-irradiated compartment with host tissue cells only or with a small tumor cell population), the immune response and specifically, the differentiation between host tissue and tumor cells, may be dependent on the arrangement of information-processing units (perceptrons). To elucidate this aspect, two different models – one with a single perceptron and a second model with two perceptrons – are investigated.

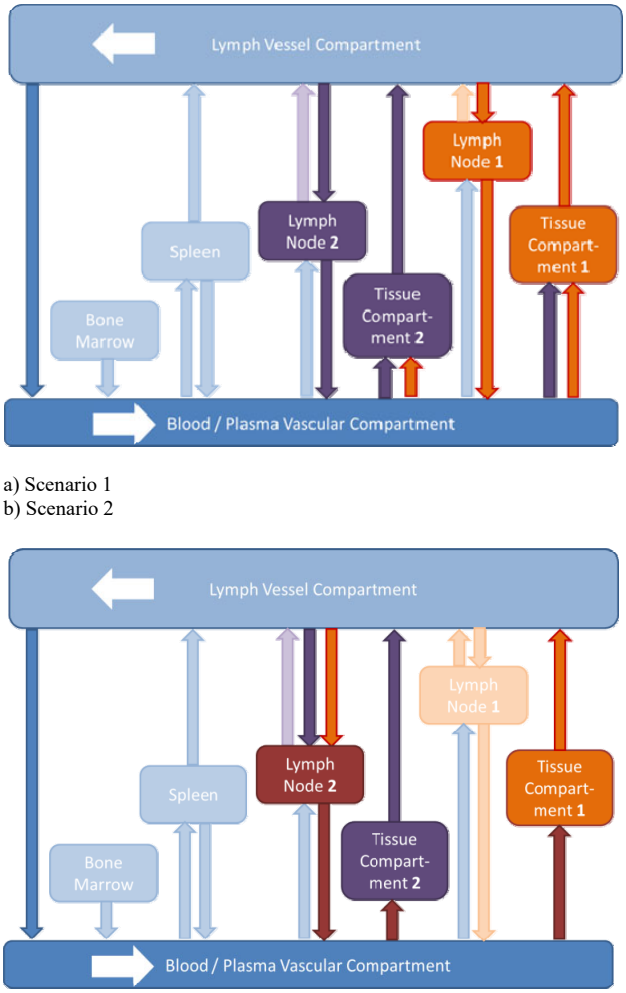

Figure 2. Circulation of antigen pattern information and corresponding effector cells: Upper diagram (a) depicts the case where two lymph nodes are separately processing the antigen pattern information from two corresponding tissue compartments (the relevant compartments are highlighted; not all lymphatic organs / tissues are shown). This implies that every compartment is drained by separated lymph vessels (parallel information processing). Assuming a mix of effector cells downstream in the lymph and blood circulation (flow direction indicated by arrows in the lymph vessel- and blood compartment), a migration of effector cells from both lymph nodes into both tissue compartments is possible, resulting in an exchange of information. In the lower diagram (b), the case of two tissue compartments with a downstream antigen pattern processing by only one lymph node is illustrated. In this case, the antigen pattern information undergoes a combined processing with the result of effector cell populations originating from the same lymph node. Flow charts are based on lymphocyte recirculation routes by Owen et al. (2013).

Material and Methods

The model used for this study is based on a model for a coupled immune-tumor-host ecosystem presented by Scheidegger et al. (2020) and Scheidegger et al., (2022). The main difference to the already existing model is the implementation of a second tumor-host compartment and the modification of the adaptive immune system model for a multi-compartment situation. Whereas the introduction of new compartments is conceptually straightforward, the adaption of the immune system part requires a mapping of the antigen-pattern – detecting and classifying unit (perceptron) to the biological system. In this study, two different scenarios for this mapping are presented (Fig.2). These scenarios are based on the circulation of antigens and immune system cells (APC's, effector cells) in the body.

In scenario 1 (Fig.2a), the two tissue compartments are connected to two different lymph nodes, each receiving antigen information only from the connected tissue compartment. Assuming a mix of effector cells downstream in the lymph and blood circulation, a migration of effector cells from both lymph nodes into both tissue compartments is possible, resulting in an exchange of information. In scenario 2 (Fig.2b), the two tissue compartments are connected via the lymph vessel compartment to a joint lymph node. In this scenario, the antigen pattern information is processed only in one lymph node, resulting in effector cell populations originating from the same lymph node.

Fig.3 depicts the translation of the two scenarios described in Fig.2 to the model structure consisting of tissue compartments (tumor-host ecosystems) and an antigen-processing unit (perceptron). In both tissue compartments, the same antigen patterns for the corresponding host- and tumor cell populations are used (in Fig.3, the patterns are depicted by 3x3 matrices, representing an antigen pattern vector; green for host tissue, blue for tumor sub-clones). To have a comparable situation to the simulations presented by Scheidegger et al., 2022, the same mutation tree for tumor cells is used.

In both compartments, the dynamic interaction between the different tumor sub-clones $T_{ik}^{(1,2)}$, host tissue $H^{(1,2)}$ and effector cells is given by the following system of ordinary differential equations:

$$\frac{dT_{11}^{(1,2)}}{dt} = (k_{T11} - k_{mut} - k_{eT} - r_{11}^{(1,2)} k_{IT} - k_{HT} H^{(1,2)} - k_{TT} T^{(1,2)} - (\alpha_T + 2\beta_T \Gamma) \cdot R^{(1,2)}) \cdot T_{11}^{(1,2)}$$

$$\frac{dT_{ik}^{(1,2)}}{dt} = (k_{Tik} - k_{eT} - r_{ik}^{(1,2)} k_{IT} - k_{HT} H^{(1,2)} - k_{TT} T^{(1,2)} - (\alpha_T + 2\beta_T \Gamma) \cdot R^{(1,2)}) \cdot T_{ik}^{(1,2)} + k_{mut} \cdot q_{il} T_{lk}^{(1,2)} \quad (1)$$

$$\frac{dH^{(1,2)}}{dt} = (k_{aH} - k_{eH} - r_H^{(1,2)} k_{IH} - k_{bH} H^{(1,2)} - k_{TH} T^{(1,2)} - (\alpha_H + 2\beta_H \Gamma) \cdot R^{(1,2)}) \cdot H^{(1,2)}$$

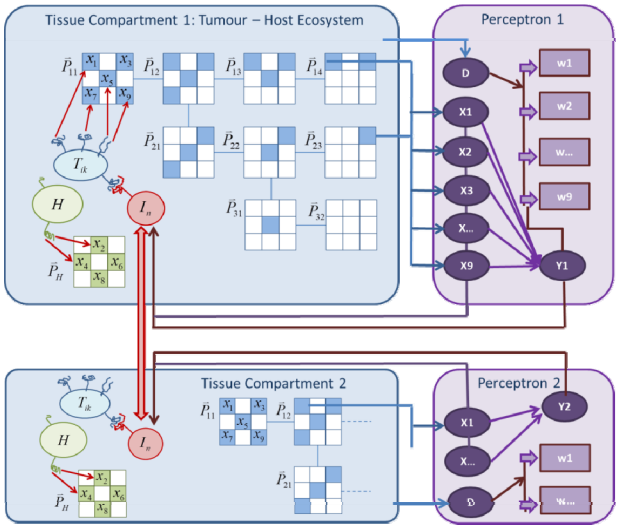

a) Scenario 1
b) Scenario 2

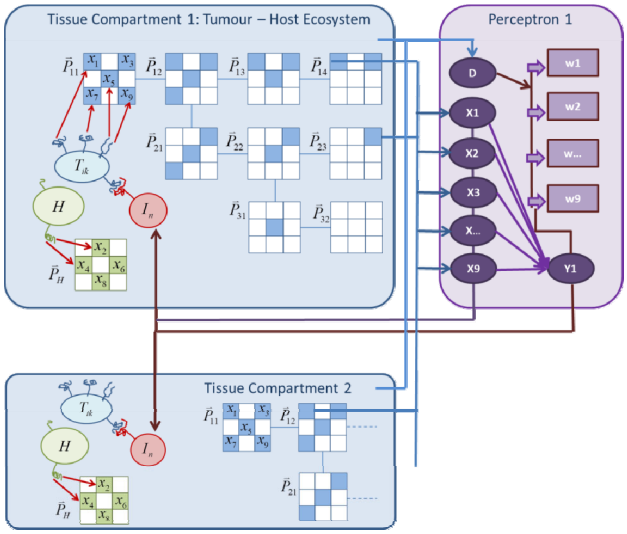

Figure 3. Model structures connecting two different tissue compartments to one or two perceptrons for antigen pattern recognition and classification: (a) two perceptrons and parallel processing according to Fig.2a, the information exchange occurs via effector cell migration (red arrow between the effector cell populations I_n); (b) case with one perceptron corresponding to Fig.2b. The perceptron 1 receives danger signals D and antigen pattern information (X_i) from both tissue compartments. Due to simplicity, not all connections (information flows, thin arrows) and elements (e.g. antigen patterns in tissue compartment 2) are shown. In case of identical antigen patterns in both tissue compartments, the cells (H = host tissue, T_{ik} = tumour sub-clone, I_n = effector cells) are the same, but the population sizes are different. Therefore, the number of cells in a specific population has to be distinguished for the two compartments (e.g. $H^{(1)}$ for host tissue in compartment 1 and $H^{(2)}$ for host tissue in compartment 2). Diagrams are based on Scheidegger et al., 2021, modified and adapted for a two-compartment / two-perceptron model.

There, $k_{Tik} \cdot T_{ik}^{(1,2)}$ is the reproduction rate of the tumor sub-population ik ($T_{ik}^{(1)}$ is the corresponding population in compartment 1 and $T_{ik}^{(2)}$ the population in compartment 2); $k_{eT} \cdot T_{ik}^{(1,2)}$ represents a spontaneous rate of cell elimination ($k_{eH} \cdot H^{(1,2)}$ for host tissue in the two compartments); the immune-system – related elimination rate is calculated by $r_{ik}^{(1,2)} k_{IT} \cdot T_{ik}^{(1,2)}$ with an interaction coefficient k_{IT} , $r_{ik}^{(1,2)}$ defines the match with antigen-receptor binding sites. For host tissue, a different coefficient k_{IH} is used; $k_{mut} \cdot q_{il} T_{lk}^{(1,2)}$ gives the rate of mutation (q_{il} is a matrix representing the topology of the population network, see Scheidegger et al., 2020). Competition between the different tumor sub-populations is included by $k_{TT} T^{(1,2)} \cdot T_{ik}^{(1,2)}$ (with the total amount of tumor cells $T^{(1,2)}$ in each of the two compartments) and for host tissue by $k_{TH} T^{(1,2)} \cdot H^{(1,2)}$; $k_{bH} \cdot H^{(1,2)} \cdot H^{(1,2)}$ represents the self-inhibition of host tissue growth. For radiation – induced cell killing, a dynamic linear-quadratic (LQ) model with a transient biological dose equivalent Γ is used, which is described in detail in Scheidegger et al., 2021 or Scheidegger et al., 2020. In this study, only compartment 1 is assumed to be treated by radiation (main tumor). Parameters and fractionation schedules are identic to the simulations presented by Scheidegger et al., 2022. Compartment 2 is assumed to be a host compartment with a metastasis. Therefore, the radiation dose rate $R^{(2)}$ is set to 0 for compartment 2.

According to the model presented by Scheidegger et al., 2022, the danger signal generation for each compartment includes a two-step process starting with lethally damaged cells which subsequently transforms to "immune-system-activating" cell population $N_{ik}^{(1,2)}$ (necrotic tumor cells) and $N_H^{(1,2)}$ (necrotic host cells; for details, see Scheidegger et al., 2022). In this study, the danger signal is calculated for each compartment separately by:

$$D^{(1,2)} = \frac{\left[\sum_{i,k} N_{ik}^{(1,2)} + N_H^{(1,2)}\right]^2}{L_{act}^2 + \left[\sum_{i,k} N_{ik}^{(1,2)} + N_H^{(1,2)}\right]^2} \tag{2}$$

L_{act} governs the steepness of this sigmoidal relation between the amount of necrotic cells and the danger signal D and is assumed to be the same for both compartments.

Scenario 1

Every cell of a specific cell population (tumor sub-clones and host tissue) bears a corresponding pattern (in Fig.3 represented by 3x3-matrices), which is defined by the elements of the antigen pattern vector $\bar{P}_{ik}$ for each compartment. The presence of a component in this pattern vector is considered to be dependent on the amount of cells bearing this specific component. Considering the amount of antigens in a compartment, a second antigen pattern vector $\bar{X}^{(1,2)} = X_i^{(1,2)}$ can be calculated for each compartment (1,2) separately: According to Fig.3, the antigen signal strength of the first component for example is given by:

$$X_1^{(1,2)} = \frac{\left(\tilde{T}_{11}^{(1,2)} + \tilde{T}_{12}^{(1,2)} + \tilde{T}_{13}^{(1,2)} + \tilde{T}_{14}^{(1,2)}\right)^2}{\left(X_{act}\right)^2 + \left(\tilde{T}_{11}^{(1,2)} + \tilde{T}_{12}^{(1,2)} + \tilde{T}_{13}^{(1,2)} + \tilde{T}_{14}^{(1,2)}\right)^2} \tag{3}$$

with $\tilde{T}_{ik}^{(1,2)} = T_{ik}^{(1,2)} + \eta N_{p,ik}^{(1,2)} + \chi N_{ik}^{(1,2)}$: pre-necrotic and necrotic cells are considered to contribute to the presence of antigens, but with the weighting factors η and χ (for details, see Scheidegger et al., 2022). X_{act} influences the sigmoidal activation response. For each compartment, a separated perceptron is used to adapt the corresponding antigen weights $w_i^{(1,2)}$ for generating the perceptron response by comparing the actual danger signal strength $D^{(1,2)}$ with the perceptron response $Y^{(1,2)}$:

$$\frac{dw_i^{(1,2)}}{dt} = a \cdot (D^{(1,2)} - Y^{(1,2)}) \cdot X_i^{(1,2)} \tag{4}$$

with the perceptron response $Y^{(1,2)}$:

$$Y^{(1,2)} = \frac{\left(\Sigma^{(1,2)}\right)^{\xi}}{Y_{act}^{\xi} + \left(\Sigma^{(1,2)}\right)^{\xi}} \tag{5}$$

where $\Sigma^{(1,2)}$ denotes the sum of the antigen signals in each compartment:

$$\Sigma^{(1,2)} = \sum_{i=1}^{9} w_i^{(1,2)} X_i^{(1,2)} \tag{6}$$

Technically, the sigmoidal response function does not correspond to a perceptron but to a sigmoidal neuron. Since the immune system does not have neurons in the biological sense, the term "perceptron" is used. The activation parameter Y_{act} is assumed to be the same for both perceptrons. The production is governed by the perceptron responses $Y^{(1,2)}$ of each perceptron. Since in this scenario, the effector cell population will be mixed during migration to the target compartment, the effector cell population growth rate is given by $k_I \cdot (Y^{(1)} X_n^{(1)} + Y^{(2)} X_n^{(2)}) / 2$ for both compartments. The match of antigen pattern with the effector cell population vector $I_n = \bar{I}$ is evaluated by the dot product between $\bar{I}$ and an antigen pattern vector $\bar{P}$ with components = 1 for bearing a specific antigen corresponding to the antigen pattern vector component X_n and 0 otherwise: $r_{ik}^{(1,2)} = \bar{I}^{(1,2)} \bullet \bar{P}_{ik}$. The spontaneous elimination of effector cells is considered by the elimination rate constant k_{eI} and – only for compartment 1 - the radiation-induced elimination by a dynamic LQ model with effector-cell specific radio-sensitivity coefficients α_I and β_I . It is important to keep in mind, that only the immune (effector) cells in the tumor compartment are irradiated and the radiation dose rate in compartment 2 is set to $R^{(2)} = 0$. Summing up these rates, the temporal change of effector cell population can be calculated by:

$$\begin{aligned} \frac{dI_n^{(1,2)}}{dt} &= \frac{k_I}{2} \cdot (Y^{(1)} X_n^{(1)} + Y^{(2)} X_n^{(2)}) \\ &- (k_{eI} + (\alpha_I + 2\beta_I \Gamma_I) \cdot R^{(1,2)}) \cdot I_n^{(1,2)} - k_{IT} \cdot \left(\sum_{i,k} r_{ik}^{(1,2)} T_{ik}^{(1,2)}\right)_n \end{aligned} \tag{7}$$

Scenario 2

In the scenario with one joint lymph node, the danger signals from each compartment contribute equally to a combined danger signal by: $D = (D^{(1)} + D^{(2)})/2$. The antigen pattern vector $\vec{X}^{(1,2)} = X_i^{(1,2)}$ is calculated similar to scenario 1. Assuming a mixture of (presented) antigens in a lymph node, the two separated antigen pattern vectors contribute to a combined vector $X_i = (X_1^{(1)} + X_1^{(2)})/2$. The calculation of the corresponding antigen weights w_i for generating the perceptron response by comparing the actual danger signal strength D with the perceptron response Y is similar to the model presented by Scheidegger et al., (2020):

$$\frac{dw_i}{dt} = a \cdot (D - Y) \cdot X_i \tag{8}$$

with the unique perceptron response Y:

$$Y = \frac{\Sigma^{\xi}}{Y_{act}^{\xi} + \Sigma^{\xi}} \tag{9}$$

where Σ denotes the sum of the combined antigen signals:

$$\Sigma = \sum_{i=1}^{9} w_i X_i \tag{10}$$

The perceptron response Y directly governs the production of effector cells by the production rate $k_I Y X_n$ (same response for both compartments). The match of antigen pattern with the effector cell population vector $I_n^{(1,2)} = \vec{I}^{(1,2)}$ in each compartment is similar to scenario 1, but with modified effector cell population growth rate:

$$\frac{dI_n^{(1,2)}}{dt} = k_I Y X_n - (k_{eI} + (\alpha_I + 2\beta_I \Gamma_I) \cdot R^{(1,2)}) \cdot I_n^{(1,2)} - k_{IT} \cdot \left(\sum_{i,k} r_{ik}^{(1,2)} T_{ik}^{(1,2)} \right)_n \tag{11}$$

Parameter Values and Initial Conditions

In principle, the two tumor – host compartments represent a similar system, but compartment 2 is assumed to have only one tumor cell as initial value ($T_{11}^{(2)}(0) = 10^{-9}$; population sizes and constants are calibrated to 1 = 10^9 cells). Therefore, compartment 2 can be considered as a tissue compartment with a metastasis. The other initial population sizes are identical to Scheidegger et al., 2022: $H^{(1,2)}(0) = 250$, $T_{11}^{(1)}(0) = 10^{-3}$ and 0 for all other populations. Growth-, elimination- and radio-sensitivity parameters constants, application of RT starting on day 570 as well as numerical integration / time increment size and duration (1800 day) of simulation in this study are identical to those used in Scheidegger et al., 2022.

Results

In Fig.4, the temporal development of host and tumour cell populations in both compartments is displayed for scenario 1 and 2 as well as for a modified scenario 1 without effector cell exchange or mixing between the two tissue compartments (middle diagram).

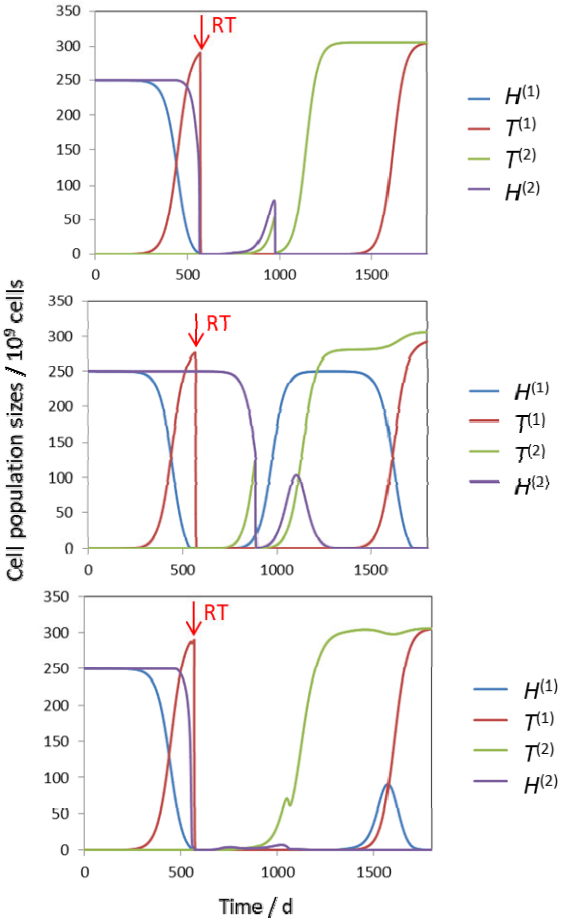

Figure 4. Host tissue ($H^{(1,2)}$) and tumor cell populations ($T^{(1,2)}$: total number of tumor cells) for the two scenarios (upper and lower graphs) and a scenario with uncoupled compartments (scenario 1 without mixing of effector cells between the compartments; middle diagram): In all displayed cases, the compartment 1 is treated by a fractionated radiation therapy (RT) with 32 fraction, each fraction with a radiation dose of 2 Gy (5x2 fractions per week), starting on day 570.

In the case without mixing effector cells (middle diagram, Fig.4), the populations of compartment 1 behave identically to the single-compartment model presented by Scheidegger et al., 2022, and can be used for comparison (as a reference), since this part of the model fully corresponds to the single compartment model and the same RT is applied (32 fractions, 2 Gy per fraction, starting on day 570). The development of

populations in compartment 2 corresponds to the case of a non-treated (non-irradiated) tissue compartment with metastasis. Compared to this case (middle diagram), the coupling of the 2 compartments by mixing the effector cell populations (scenario 1, upper image in Fig.4), the host tissue in compartment 1 is suppressed whereas the main tumour in compartment 1 exhibit a similar development. Regarding the development of the perceptron weights in Fig.5, the perceptron weights of perceptron 1 (corresponding to danger signals and antigen pattern presence in compartment 1) exhibit a separation which – in case of the uncoupled case – results in negative weights for the host tissue (as observed in Scheidegger et al., 2022). This effect disappears for the coupled case (mixing of effector cells). The weights of perceptron 2 (corresponding to compartment 2) are higher and in the uncoupled case, the host tissue weights (even weights) are above the tumour weights (odd weights). The mixing of effector cells in scenario results in a pronounced suppression of the host tissue population in compartment 1 after application of RT. In addition, the mixing of effector cells generates an abscopal effect of RT to the host tissue in compartment 2, which is induced by the application of RT in compartment 1. Regarding the tumour population in compartment 2, this population reaches the equilibrium level faster ($306 \cdot 10^9$ cells, this is similar for both compartments and based on the selection of the speed constants, see Scheidegger et al., 2022).

Similar effects can be observed for scenario 2 (lower graph of Fig.4): The suppression of the host tissue in compartment 2 is even more pronounced after RT and the metastatic tumor population in compartment 2 develop slightly faster. In contrast to scenario 1, the host population in compartment 2 exhibits a growth phase after day 1300 but decreases after day 1600. This corresponds to the growth of the tumor population in compartment 1 and a rise of the perceptron weight of the host population (Fig.5, lower graph). An interesting feature is the temporal development of the perceptron weights in scenario 2: Compared to scenario 1, the host-tissue – related (even) perceptron weights increase more after RT application but then decreases to lower values around day 1000. During the second growth phase of the main tumor in compartment 1, the host-tissue related weights increase again and show less separation to the tumor-related weights of perceptron 1 in scenario 1.

Discussion and Conclusions

Summarizing the results displayed in Fig.4, scenario 1 as well as scenario 2 exhibits a disadvantageous situation compared to the scenario with uncoupled compartments (Fig.4, middle diagram). Dependent on the temporal development of the different cell populations, the perceptron-weight - mediated responses lead to tumour – and host – tissue suppression. Preclinical and, in some extend, clinical research demonstrated that radiotherapy (RT) is able to modulate anti-tumour immune responses (Alfonso et al., 2020; Di Maggio et al., 2015; Frey et al., 2017; Frey et al., 2012). In several studies, tumour supressing - and promoting effects of RT have been found (summarized in Rückert et al., 2021). In this study, tumour-promoting effects are caused by the anti-host immune response and subsequent lack of competition – it is a question of the dynamic interplay in and between the two tissue compartments. This raises the question about the importance of this effect for anti-cancer treatments. Despite the unrealistic anti-host host response in compartment 2 observed in this study, combined ecosystem dynamics turned out as an important aspect in all tested scenarios.

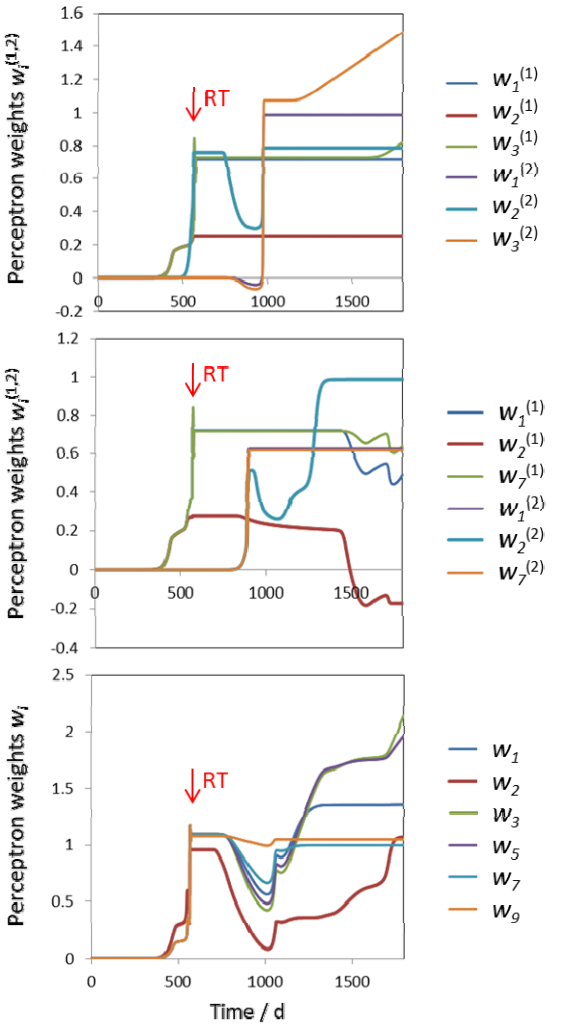

Figure 5. Temporal development of perceptron weights $w_i^{(1,2)}$ respectively w_i for the two scenarios (upper and lower graphs) and a scenario with uncoupled compartments (scenario 1 without transfer of effector cells between the compartments; middle image): Compartment 1 is treated by a fractionated radiation therapy (RT) as in Fig.4. For the even weights (i={2,4,6,8}), only w2 respectively $w_2^{(1,2)}$ is displayed since these weights behave identically due to the symmetry of the host tissue pattern. Due to clarity, only selected, representative odd weights (tumor-related weights) are shown.

In addition, the results indicate an influence of the arrangement of information-processing units (perceptrons). Translated to a real patient, this would imply the importance of the spatial arrangement of lymph nodes and vessels (understood in the sense of topological connectivity) for an optimal adaptive immune response.

The presented simplistic model structure does not allow for a perfect differentiation (classification) between tumor and host tissue. In a real (biological) immune system, a large number of interactions via co-receptors and co-factors as well as immune check-points seem to be needed to get a more specific anti-tumor response. The inclusion of several co-factors and co-receptors may be covered by more complex neural network – like structures. The topology of such a network could be inspired by the spatial interaction of the different sensing and antigen-presenting immune cells in specific micro-environments. Regarding a "local" neural network representing the information processing of multiple co-factors, danger signals and antigen-antibody or antigen-receptor bindings, such a network may be considered as "fully connected". These "local" networks may interact with each other network or with a part of them. The layers in such a combined network representing the information processing in the entire immune system cannot be assumed to be fully connected, since the information processing occurs at different sites (e.g. lymph nodes and tissue compartments) and probably not all network node responses will be fed to every node of the subsequent layer. Instead of a single perceptron which is related to the interaction of immune cells in a corresponding lymph node as suggested in this study, networks of locally interacting units may be considered as layers building a many-layer convolutional network structure. We emphasize our careful avoidance of the term "deep convolutional neural network". The notion of this specific type of neural network implies a number of specific features; whether the immune system exhibits them is subject to further investigations. However, mapping the different parts (information-processing structures) of the immune system to the topology of such neural network – like structures may be a pivotal step for getting a better insight into the principles of the immune-ecosystem dynamics in real biological systems.

References

Alfonso, J.C.L., Papaxenopoulou, L.A., Mascheroni, P., Meyer-Hermann, P., Hatzikirou, H. (2020). On the Immunological Consequences of Conventionally Fractionated Radiotherapy. *iScience* 2020, 23:100897, https://doi.org/10.1016/j.isci.2020. 100897.

Chrobak, J.M., Herrero, H. (2011). A mathematical model of induced cancer-adaptive immune system competition. *J. Biol. Sys.* 19(3): 521-532. DOI: 10.1142/S0218339011004111

Di Maggio, F., Di Maggio, M., Minafra, L., Forte, G.I., Cammarata; F.P., Lio, D., Messa, C., Gilardi; M.C., Bravatà, V. (2015). Portrait of inflammatory response to ionizing radiation treatment. *Journal of Inflammation*, 12(14), DOI 10.1186/s12950-015-0058-3.

Du, S.Q., Yuan, W. (2020). Mathematical modeling of interaction between innate and adaptive immune responses in COVID - 19 and implications for viral pathogenesis. *J. Med. Virol.* 92:1615-1628.

Frey B., Rückert M., Deloch L., Rühle P.F., Derer A., Fietkau R., Gaipl U.S. (2017): Immuno-modulation by ionizing radiation-impact for design of radio-immunotherapies and for treatment of inflammatory diseases. *Immunol. Rev*. 80(1):231-248.

Frey B., Rubner Y., Wunderlich R., Weiss E.M., Pockley A.G., Fietkau R., Gaipl U.S. (2012): Induction of Abscopal Anti-Tumor Immunity and Immunogenic Tumor Cell Death by Ionizing Irradiation – Implications for Cancer Therapies. *Current Medicinal Chemistry*, 19(12):1751-1764.

Leon, C., Tokarev, A., Bouchnita, A., Volpert, V. (2023). Modelling of the Innate and Adaptive Immune Response to SARS Viral Infection, Cytokine Storm and Vaccination. *Vaccines*, 11:127. DOI: 10.390/vaccines11010127

Owen, J. A., Punt, J., Stranford, S. A., & Jones, P. P. (2013). *Kuby Immunology* (7th ed.). W. H. Freeman & Company, New York, U.S.A.

Rosado, M.M., Pioli, C. (2020): Cancer-host battles: measures and countermeasures in radiation-induced caspase activation and tumor immunogenicity. *Cell. Mol. Immunol.*, 17:1022–1023. https://doi.org/10.1038/s41423-020-0513-9

Rückert M., Flohr A.S., Hecht M., Gaipl U.S. (2021). Radiotherapy and the immune system: More than just immune suppression. *Stem Cells*. 2021 Sep;39(9):1155-1165. doi: 10.1002/stem.3391. Epub 2021 May 18. PMID: 33961721.

Scheidegger S., Mingo Barba S., Fellermann H., Gaipl, U.S. (2022). Influence of the Antigen Pattern Vector on the Dynamics in a Perceptron-based Artificial Immune - Tumour- Ecosystem during and after Radiation Therapy. In: Schneider J.J., Weyland M.S., Flumini D., Füchslin R.M. (eds), Artificial Life and Evolutionary Computation. WIVACE 2021. Communications in Computer and Information Science, Springer, Cham, https://doi.org/10.1007/978-3-031-23929-8

Scheidegger S., Mingo Barba S., Gaipl U.S. (2021). Theoretical Evaluation of the Impact of Hyperthermia in Combination with Radiation Therapy in an Artificial Immune-Tumor-Ecosystem. *Cancers*, 13:5764. DOI: 10.3390/cancers13225764

Scheidegger S., Mikos A., Fellermann H. (2020). Modelling Artificial Immune – Tumor Ecosystem Interaction During Radiation Therapy Using a Perceptron – Based Antigen Pattern Recognition. ALIFE 2020: The 2020 Conference on Artificial Life July 2020, The MIT Press Journals, pages 541-548.

Wyatt A., Levy D. (2020). Modeling the Effect of Memory in the Adaptive Immune Response. Bulletin of Mathematical Biology, 82:124. DOI: 10.1007/s11538-020-00798-9